THE EUROPEAN
PHYSICAL JOURNAL
SPECIAL TOPICS

Regular Article

Characteristics of the specific brain functional network correlate with the latency of motor imagery

Oxana Drapkina[1,a], Andrey Savosenkov[2,3,b], Susanna Gordleeva[1,2,3,c], Semen Kurkin[3,d], Artem Badarin[1,3,e], Nikita Grigorev[2,3,f], Anna Udoratina[2,g], Anton Kiselev[1,h], Victor Kazantsev[1,2,3,i], and Alexander Hramov[2,3,j]

[1] Coordinating Center for Fundamental Research, National Medical Research Center for Therapy and Preventive Medicine, 10 Petroverigsky per., Moscow 101990, Russia

[2] Neurodynamics and Cognitive Technology Laboratory, Lobachevsky State University of Nizhny Novgorod, 23 Gagarin Avenue), Nizhny Novgorod 603022, Russia

[3] Baltic Center for Artificial Intelligence and Neurotechnology, Immanuel Kant Baltic Federal University, 14 Alexander Nevsky Street, Kaliningrad 236016, Russia

Abstract Motor imagery is a widely used technique in neurophysiological research and brain–computer interface applications for restoring lost motor functions. This study aimed to analyze the neural correlates of motor imagery at the level of brain functional networks using electroencephalography (EEG). Thirty subjects performed motor executions, quasi-movements, and imaginary movements while EEG data were recorded. We explored the correlation between the latency of motor imagery and the characteristics of brain functional networks in the alpha- and beta-frequency ranges. The analysis revealed a number of nodes within the network whose local cluster coefficients negatively correlated with the time of motor imagination onset. This indicates that a decrease in the corresponding networks metrics would lead to improved rate of motor imagination. These nodes were predominantly located in the frontal cortex, parietal, and temporal lobes. The identified nodes, particularly the Frontal Mid L zone, hold promise as potential targets for non-invasive brain stimulation techniques such as transcranial magnetic stimulation or transcranial direct current stimulation. Stimulating these areas may enhance motor imagination ability and facilitate the rehabilitation process, especially for stroke patients with severe motor impairment.

1 Introduction

According to the trends in neuroscience, a large number of modern studies are devoted to the phenomenon of motor imagery (MI) [1]. It is the state during which motor acts are mentally reproduced in working memory without any overt motor output [2]. This technique has become most popular in combination with non-invasive brain–computer interfaces (BCIs), often utilizing EEG. The use of such BCIs is a promising direction in restoring lost motor functions [3–6]. In the context of motor activity rehabilitation, BCI systems are able to recognize a patient's attempt to move. However, the severity of the disorder often hampers the operator's interaction with the neurointerface. It is supposed to use non-invasive techniques, such as functional electrical stimulation or transcranial magnetic stimulation (TMS), to overcome such problem. Nevertheless, the challenge of selecting the

[a] e-mail: drapkina@bk.ru

[b] e-mail: andrey.savosenkov@gmail.com

[c] e-mail: gordleeva@neuro.nnov.ru

[d] e-mail: kurkinsa@gmail.com (corresponding author)

[e] e-mail: badarin.a.a@mail.ru

[f] e-mail: grigorev.na@unn.ru

[g] e-mail: udoratina@unn.ru

[h] e-mail: kiselev@gnicpm.ru

[i] e-mail: kazantsev@neuro.nnov.ru

[j] e-mail: hramovae@gmail.com

most impactful stimulation site to improve the qualitative characteristics of MI and interaction with BCI remains unsolved.

Changes in brain rhythms during MI performance may serve as the discriminating characteristics of brain areas. Motor imagery is primarily accompanied by the desynchronization of mu- and beta-rhythms in the sensorimotor areas of the cortex [7, 8]. Global synchronized activity in the theta range is also observed during the initiation phase of imaginary movements [9, 10]. Furthermore, desynchronization of the mu-rhythm correlates positively with the increase in corticospinal excitability [11–14]. It may indicate the success in the reproduction of motor images and the greatest contribution to the rehabilitation procedures using this paradigm [6, 15–17].

The primary focus in studying the neural mechanisms of motor imagery is investigating the brain areas involved in forming the ideomotor act. Many brain regions are associated with MI performance. Activation sites are present in the premotor cortex (PMC), supplementary motor area (SMA), and lower parietal lobes, including the intraparietal sulcus (IPS). But mostly, MI is associated with the motor cortex. Interestingly, the primary motor cortex (M1) shows only about 30% of the activation observed during real motor execution, and the activation site is located more anteriorly in the precentral gyrus [1, 18]. Although various zones have been studied for mapping and influencing the processes of MI formation, many studies have predominantly focused on the primary motor cortex. They utilized methods, such as TMS and electrical stimulation (tDCS), to non-invasively alter cortical excitability. These studies demonstrate the relationship between the primary motor cortex activation and the performance of the MI task [19], the degree of event-related desynchronization during motor imagery [11], as well as changes in muscle activity [20]. As in the TMS studies, a tDCS session for the primary motor cortex before applying MI-BCI significantly improved test scores in a group of stroke patients [21].

Functional networks (FNs) [22, 23] emerging during MI are also being investigated [24–26]. The role of the motor cortex and the connectivity between the superior parietal lobule and the supplementary motor area in kinesthetic and visual motor imagery has been explored [27]. Additionally, the connectivity between the SMA and other brain regions during MI performance has been discovered [28]. However, the correlation between specific MI characteristics and the activity of brain FN has not been thoroughly examined. Such investigations will make it possible to identify the FN nodes, the impact on which could change the characteristics of the MI (e.g., reduce the latency of MI) through external influences (e.g., TMS).

This study is aimed at the analysis of motor imagery mechanisms at the level of the brain functional networks. To do this, we reconstruct the neural sources and FNs using EEG data. Based on network analysis, we identify the brain areas that influence the characteristics of MI.

2 Materials and methods

2.1 Subjects

The study comprised 30 subjects (21 women) aged 18 to 34 years, with a mean age of 20.93 ± 2.14—mean ± standard deviation). None of the subjects had a previous psychiatric or neurological history. Based on the Edinburgh inventory, all subjects had a right-dominant hand score of 0.77 ± 0.18 (mean ± standard deviation). The study received approval from the local ethics committee and was conducted in accordance with the Declaration of Helsinki. Informed consent has been obtained from all subjects involved in the study.

2.2 Experimental design

The experimental session began with the subjects undergoing a test to determine their dominant hand. Subsequently, EEG electrodes were placed on the subject's head according to the "10–10" scheme (32 channels: Fp1, Fp2, F3, Fz, F4, Fc1, Fc2, F7, Ft9, Fc5, F8, Fc6, Fc10, T7, Tp9, T8, C3, Cz, C4, Cp5, Cp1, Cp2, Cp6, Cp10, P7, P3, Pz, P4, P8, O1, Oz, O2). At the same time, the subject received instructions about the structure of the experiment and the performance of quasi-movements and imaginary movements. EEG was carried out using Ag/AgCl electrodes connected to an NVX-52 amplifier (MKS, Zelenograd, Russia). The resistance at all electrodes was below 15 kΩ, and the recording was performed at a sampling rate of 1 kHz.

Next, the experiment began with the EEG recording, and the stages of the experiment were predefined (Fig. 1) and controlled by the computer program. After a 3 min recording of background activity (baseline), motor executions (ME) were performed, followed by quasi-movements (QM), and a series of imaginary movements (MI). We used such a sequence of tasks for the facilitation of quality performance by the participants of kinesthetic motor imagery. Rest intervals of 2 min (rest) was provided between tasks. Finally, another recording of background activity (baseline 2) was conducted.

Each series of movements consisted of 20 trials. The trial consisted of making the corresponding hand movement for 5 s ("motor task"), followed by a 5-second pause between successive movements (Fig. 1). Instructions regarding
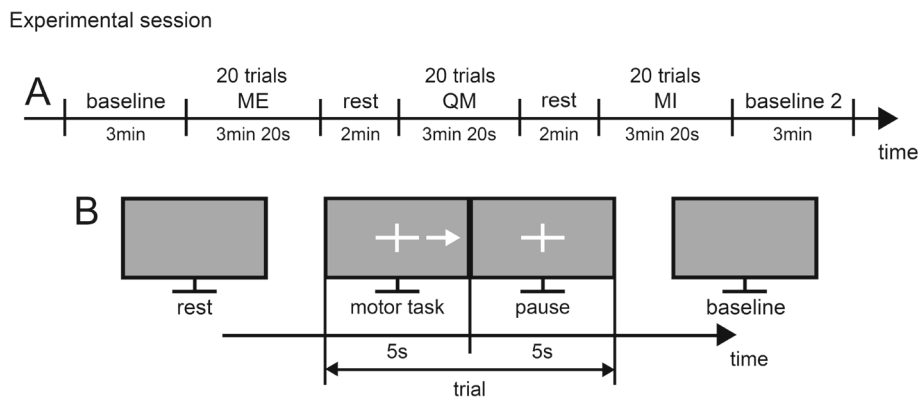
Fig. 1 Design of the experiment. **A** Timeline of the experiment session. **B** The typical sequence of the visual cues and the structure of one trial. ME–motor execution, QM– quasi-movements, MI–imaginary movements

the tasks to be performed were presented to the subjects as a visual stimulus in the form of a cross with an arrow (known as the "arrow paradigm" [29]) displayed on a 27-inch monitor positioned 2 ms away from the subject at eye level.

2.3 Preprocessing of EEG

The EEG data underwent signal processing to eliminate power line interference at 50 Hz and its harmonics. This was achieved by employing a band-stop Butterworth filter with a range of [49.5, 50.5] Hz. Furthermore, to minimize the impact of different sources of noise and physiological artifacts, a band-pass Butterworth filter was utilized within the range of [1, 70] Hz. Considering that eye movements and cardiac activity can disrupt the desired frequency range of the EEG signals (1–30 Hz), an independent component analysis (ICA) was employed to effectively eliminate these unwanted artifacts [30].

2.4 Epoching of data and sensor-level analysis

Based on the knowledge regarding the specific dynamics of brain rhythms during MI tasks, time intervals of interest (TOIs) and frequency ranges were selected for further analysis at the source level. Theta (4–8 Hz), alpha (10–14 Hz), and beta (14–30 Hz) frequency ranges were considered. The following TOIs were chosen for analysis: the pause interval between successive executions of movements (Pre, $0.5-4.5$ s, time is indicated relative to one trial, see Fig. 2); the first 0.5 s after the command (Post1, $5-5.5$ s); 2 s interval during movements imagination (Post2, 6–8 s). It is known that within the first approximately 0.5 s after the command to perform a movement (both real and imaginary), a synchronization (increase) of the theta rhythm is observed. This reflects the process of sensorimotor integration resulting from the reaction to the stimulus and preparation for executing the movement [9]. Subsequently, there is a desynchronization (decrease) of alpha- and beta-rhythms in the motor and frontal cortices. Such rhythm dynamics correspond to the process of an imaginary movement performing. In this study, we will further consider the Post2 interval, as it encompasses processes related to the execution of the motor task.

To validate the chosen TOIs, the sensor-level analysis was performed. The power of the wavelet spectrum was calculated using the Morlet basis function for the selected EEG TOIs and frequency ranges. For each subject, the wavelet power was averaged over the respective time and frequency ranges and across 20 trials of the imaginary movement series. The obtained wavelet power distributions (topograms) in the group of subjects were compared using a statistical t test for paired samples, specifically for the Post- versus Pre-intervals, in the theta, mu, and beta ranges (see Fig. 2). Statistical significance was corrected for multiple comparisons using a permutation cluster-based test with Monte Carlo randomization [31], with an alpha significance threshold of 0.025. This process resulted in clusters in power distributions in the spatial domain (along the EEG channels), indicating statistically significant power changes between the analyzed conditions.

The described above dynamics of brain rhythms are validated by the sensor-level results (see the topograms in Fig. 2) obtained through statistical comparisons of wavelet power distributions for different time intervals and frequency ranges.
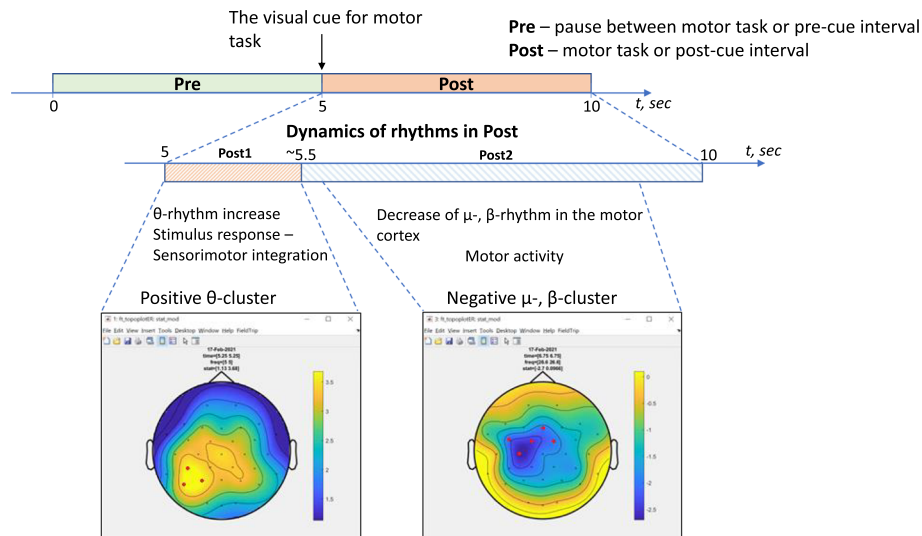
Fig. 2 Illustration of the structure of one trial during the performance of MI task and the qualitative dynamics of θ-, α-, and β-rhythms. The topograms show the results of the statistical comparisons of power distributions over the channels between post-cue ($0.5-4.5$ s or $5-5.5$ s) and pre-cue ($6-8$ s) intervals averaged over the corresponding time intervals and frequency ranges (θ- and ($\alpha+\beta$)-range); the results were obtained using the permutation cluster-based t test at the group-level; the color indicates the values of t-statistics; red points mark the channels where significant changes between Post- and Pre-intervals are observed

2.5 Reconstruction of brain functional network

Functional connections in the cortical network of the brain were determined in the source space [32] across different frequency ranges (alpha and beta) and during selected time intervals (Pre, Post2, Rest). For the source localization, we utilized the partial canonical coherence (PCC) method, which operates in the frequency domain [33]. The PCC method is better suited for estimating connections between source dipoles, since it is more flexible in terms of data processing: PCC directly derives the Fourier coefficients (amplitude and phase estimates) for each dipole, separately for each of the trials.

MRI template image of the brain "Colin27" [34] was utilized to construct a head model using the boundary element method (BEM) with three types of tissues: brain, skull, and scalp [35]. Source activity distributions were obtained on a three-dimensional grid with 12000 voxels in the brain. To map the locations of the sources to the anatomical regions of the brain, the brain atlas with automated anatomical labeling (AAL) was employed [36]. The source power was averaged over the corresponding TOIs.

We used a coherence measure to assess the strength of the connection between sources [37]. It allows to exclude more effectively false connections that are caused by the effect of field spread ("field spread" problem). Thus, to restore the functional network, the matrix of connections between all nodes (dipoles) in the brain volume is first determined. The parceling procedure is then carried out using the AAL brain atlas, resulting in a 116x116 matrix that contains coherence measures between 116 brain anatomical regions. For further analysis, we consider changes in the connection measures relative to the resting-state connectivity matrices (the so-called, "baseline correction" procedure was performed).

To identify functional connections that significantly change between compared conditions or time intervals, a network modification of a nonparametric cluster-based test (network-based statistic, NBS) was used [38], as well as the false detection rate (FDR) approach [39]. These approaches allow one to effectively solve the multiple comparisons problem at the network level. To analyze the direction of the effect between the conditions, the connections were averaged over all the links included in the corresponding identified cluster.

2.6 Estimation of the MI latency

To evaluate the efficiency of movement imagination, we estimated the latency of MI in the form of average brain response time. We made it due to the peculiarities of motor imagination since the very moment of MI beginning cannot be registered using EMG or other devices: MI does not have its obvious manifestations. We proposed an original procedure for determining the response time. First, we selected 13 channels (FC5, FC1, FC2, FC6, T7, C3, Cz, C4, T8, CP5, CP1, CP2, CP6) related to the motor area. Then, the wavelet transformation with the Morlet basis function in the alpha frequency range was applied to the considered data. The acquired data were

Eur. Phys. J. Spec. Top. (2024) 233:479–488

483

trimmed over time with an offset of 0.5 s at both ends to avoid edge effects. The data corresponding to the Pre-TOI were averaged over time and used for the percentage normalization of data in the Post TOI. The resulting wavelet surfaces were averaged over frequencies. Thus, for each trial of each person, there were 13 (according to the number of channels) time series of averaged amplitudes in the upper alpha range. For the data obtained, a clustered-based one-sample t-test with permutations was used. The unit of observation was a single trial, and the test was carried out separately for each person. Before the test, the adjacency matrix of EEG channels was also calculated and used in clustering. During the test, the critical alpha level was set to 0.05. However, if it was not possible to detect significant clusters, then the level was successively reduced to values of 0.025, 0.0125, and 0.0015625. To estimate the average response time for each person, the local minimum time on t-values dependence in the first significant cluster of channels was chosen (see [10] for more detailed description of the algorithm).

2.7 Network analysis

For the estimation of the correlation between the functional connectivity strength and the time of MI initiation in the group of subjects, Pearson's correlation test with permutations was applied. For this purpose, the sets with reaction times and connection strengths were mixed separately, and the Pearson coefficient was calculated for the resulting sets. This procedure was repeated 1000 times, with the help of which the distribution of Pearson coefficient values corresponding to the null hypothesis was calculated. Then the coefficient for the original sets was calculated. If it exceeded a certain value corresponding to the critical level of the null distribution $\alpha = 0.025$, the obtained index was considered significant. The described procedure was repeated separately for each functional connection.

To characterize the topological structure of identified brain networks, we calculated the undirected weighted local clustering coefficient [40], which measures the prevalence of node clusters in a functional network.

2.8 Methods implementation

Preprocessing of EEG data, epoching, sensor-level analysis and statistics, and source-level connectivity analysis, were performed in MATLAB 2018b using FieldTrip Toolbox [41]. The estimating of the MI brain response time was made with the Python MNE package. To analyze correlations between functional connectivity measure and MI latency, we utilized the Pearson correlation test in the SciPy package. To calculate clustering coefficient, we used Brain Connectivity Toolbox [40].

3 Results

3.1 MI latency

For each subject, we assessed the average MI latency (see the group-level distribution of MI brain response time in Fig. 3). The mean time for the group was about 1.1 s.
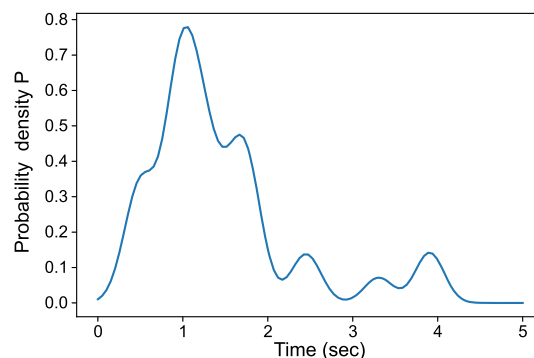

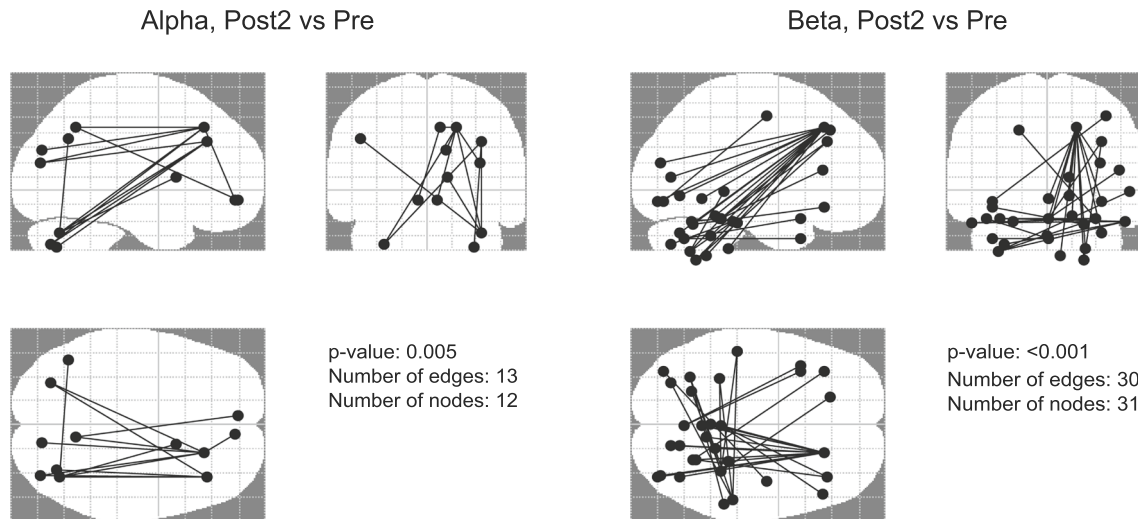**Fig. 3** The group-level distribution of MI brain response time

484

Eur. Phys. J. Spec. Top. (2024) 233:479–488

Alpha, Post2 vs Pre

Beta, Post2 vs Pre

p-value: 0.005
Number of edges: 13
Number of nodes: 12

p-value: <0.001
Number of edges: 30
Number of nodes: 31

Fig. 4 Functional connections in the coronal, axial, and sagittal projections of the brain identified using a statistical NBS t test Post2 vs. Pre at the level of the group of subjects for alpha (Left) and beta (Right) frequency ranges. The 30 most significant connections are shown

3.2 The MI-specific brain functional networks

We analyzed the brain functional networks specific to MI performance. Utilizing the statistical NBS t-test (Post2 vs. Pre), we revealed character sub-networks where the connections are stronger in the Post2 TOI compared to the Pre-TOI both in the alpha (Fig. 4, Left) and beta (Fig. 4, Right) frequency ranges. In the alpha range, 12 nodes and 13 edges were identified with a p-value of 0.005, while in the beta range, 31 nodes and 30 edges were found with a p value < 0.001. The revealed network in the alpha range includes the following main hubs: the superior and middle frontal gyri on the right, and the precuneus on the right (Precuneus_R), which reflect the activity of the central executive network. The network in the beta range includes the following main hubs: the superior frontal gyrus on the right and the inferior temporal gyrus on the right. Additionally, the motor and visual cortex regions were also involved in these networks, indicating their activation during the imagination of movements, under the control of the central executive network.

3.3 Results of correlation analysis

We carried out a correlation analysis and revealed functional networks in the alpha and beta ranges (see Fig. 5), in which changes in the strength of connections between Post–Pre-intervals, associated with the performance of MI, significantly positively correlated at the group level with the rate of MI onset. In the alpha range, the revealed network consisted of 46 nodes and 58 edges with a p value of 0.005. In the beta range, there were 20 nodes and 16 edges with a p value < 0.001. These networks are the so-called "task-positive networks" (TPNs) and include hubs from the central executive network, ventral attentional network, and elements of the motor cortex.

3.4 Analysis of the network measures

The topological consideration of the identified task-positive networks revealed their distributed structure across various brain regions, including several key nodes (hubs). We conducted a correlation analysis to reveal relationships between the changes (Post–Pre) in the nodes' clustering coefficients and the time of MI initiation. Table 1 presents the nodes (brain regions) that exhibited in the alpha frequency range significant correlations between the change in their clustering coefficients and the time of MI initiation, along with the corresponding Pearson correlation coefficients (R) and p values. These nodes were primarily located in the frontal cortex, parietal lobe, and temporal lobe. Note that all significant nodes exhibited a negative correlation. In this context, a negative correlation indicates that an increase in the clustering coefficient leads to a shorter reaction time. Therefore, to decrease the time of MI initiation, it is necessary to increase the clustering coefficient of the node characterized by a significant negative correlation.
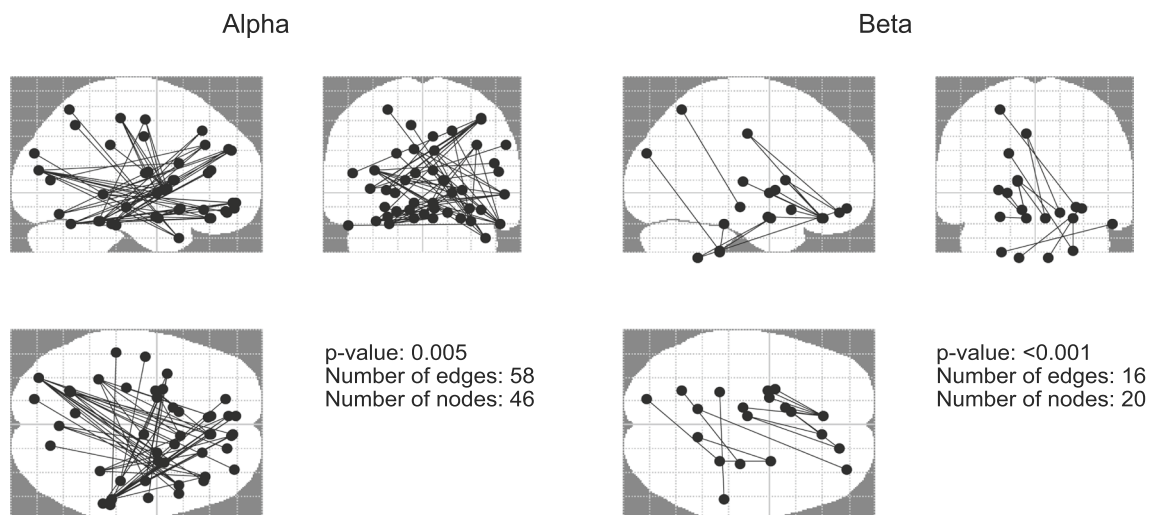
Fig. 5 Functional connections in the coronal, axial, and sagittal projections of the brain, in which changes in the strength of connections between Post–Pre-intervals significantly positively correlated at the group level with the rate of MI onset (the so-called "task-positive networks"); the networks are shown for the alpha (Left) and beta (Right) frequency ranges

Table 1 Nodes (brain areas) for which a significant correlation was found between the change in their clustering coefficients and the time of MI initiation, as well as the corresponding Pearson correlation coefficients R and p values

Band	Zone	R	p value
10–14 Hz	Amygdala_L	− 0.44673	0.014993
	Frontal_Mid_L	− 0.3363	0.043978
	Frontal_Mid_Orb_R	− 0.3658	0.029985
	Frontal_Mid_R	− 0.38251	0.023988
	Frontal_Sup_R	− 0.36091	0.046977
	Hippocampus_L	− 0.3554	0.030985
	Occipital_Mid_L	− 0.35398	0.03998
	Pallidum_L	− 0.39299	0.022989
	Postcentral_R	− 0.35109	0.021989
	Putamen_L	− 0.38232	0.033983
	SupraMarginal_R	− 0.42037	0.008996
	Temporal_Mid_R	− 0.35114	0.04098
	Temporal_Pole_Sup_L	− 0.34339	0.047976
	Thalamus_L	− 0.42799	0.004998
	Thalamus_R	− 0.3607	0.03998

4 Discussion

In this study, we investigated the correlation between the temporal characteristics of motor imagery and the activity of functional brain networks in the alpha and beta frequency ranges. Our findings revealed that certain nodes within the network, predominantly located in the frontal cortex, parietal lobe, and temporal lobes, exhibited correlations with the temporal characteristics of motor imagination. These results align with the current understanding of the activation centers involved in motor imagination [42–46]. Specifically, we focused on identifying negative correlations in these nodes, indicating an increase in the corresponding network metric, which can enhance the rate of motor imagination. The results of our study are consistent with previous research that observed a decrease in EEG activity in the mu-band during motor imagery tasks [26, 47, 48]. It has been suggested that mu (alpha) oscillations may serve as an index of successful imagery performance [49], although the relationship between response time characteristics and brain networks has not been previously explored.

486

Eur. Phys. J. Spec. Top. (2024) 233:479–488

TMS can be employed to influence the local clustering coefficient, making the identified nodes (Table 1) potential candidates for stimulation. Enhancing motor imagery characteristics is particularly important for accelerating a rehabilitation process. Studies have shown that motor imagery ability is preserved even in stroke patients with severe motor impairment and can be further improved through specialized feedback training [50]. Therefore, targeting brain regions activated during motor imagery tasks for TMS intervention in stroke patients with severe motor impairment holds promise. While some nodes may be inaccessible for TMS stimulation, alternative non-invasive techniques such as transcranial direct current stimulation (tDCS) can be considered. For example, anodal tDCS over lobule VII has been shown to modulate cortical and sub-cortical nodes involved in the execution and imagination of specific movements, leading to improved motor performance and accuracy [51]. Anodal tDCS can also enhance motor imagery performance when used as a neurofeedback tool in motor imagery tasks [52]. In more complex tasks, like postural control, tDCS has demonstrated short-term effects on motor imagery practice, particularly in individuals prone to fatigue and patients with neurological conditions [53].

The obtained results show that the Frontal Mid L zone appears to be a promising area for stimulation as it serves as an important hub in the central executive network and represents the dorsolateral prefrontal cortex (DLPFC) that is uniquely activated during motor imagery [54]. This is consistent with the results [55] where the right DLPFC and the right inferior parietal lobule (IPL) showed high activation levels during motor imagery tasks involving object manipulation. It is known that the DLPFC is associated with dynamic changes in response strategy [56]. It is related to choosing the strategies to reach the goal [57] and selecting and maintaining behaviorally relevant information [58]. Importantly, this area is highly accessible with TMS.

Based on the results obtained, we conclude that in order to activate the MI-specific functional networks, it is necessary to influence the hubs of these networks with TMS or tDCS, while it is beneficial to choose those that demonstrate a significant negative correlation with time. This is necessary in order to activate them more effectively and thereby prepare a person to complete the assigned MI task. Indeed, the recent study by Kurkin et al. [10] discovered that rhythmic transcranial magnetic stimulation of the left DLPFC speeds up the MI latency.

Data availability The data presented in this study are available on request from the corresponding author.

References

1. A.M. Ladda, F. Lebon, M. Lotze, Using motor imagery practice for improving motor performance-a review. Brain Cogn. **150**, 105705 (2021)
2. J. Decety, The neurophysiological basis of motor imagery. Behav. Brain Res. **77**(1–2), 45–52 (1996)
3. R. Mane, T. Chouhan, C. Guan, Bci for stroke rehabilitation: motor and beyond. J. Neural Eng. **17**(4), 041001 (2020)
4. Y. Miao, S. Chen, X. Zhang, J. Jin, R. Xu, I. Daly, J. Jia, X. Wang, A. Cichocki, T.-P. Jung et al., Bci-based rehabilitation on the stroke in sequela stage. Neural Plast. (2020). https://doi.org/10.1155/2020/8882764
5. M.A. Khan, R. Das, H.K. Iversen, S. Puthusserypady, Review on motor imagery based bci systems for upper limb post-stroke neurorehabilitation: from designing to application. Comput. Biol. Med. **123**, 103843 (2020)
6. N.A. Grigorev, A.O. Savosenkov, M.V. Lukoyanov, A. Udoratina, N.N. Shusharina, A.Y. Kaplan, A.E. Hramov, V.B. Kazantsev, S. Gordleeva, A bci-based vibrotactile neurofeedback training improves motor cortical excitability during motor imagery. IEEE Trans. Neural Syst. Rehabil. Eng. **29**, 1583–1592 (2021)
7. D.J. McFarland, L.A. Miner, T.M. Vaughan, J.R. Wolpaw, Mu and beta rhythm topographies during motor imagery and actual movements. Brain Topogr. **12**, 177–186 (2000)
8. G. Pfurtscheller, C. Brunner, A. Schlögl, F.L. Da Silva, Mu rhythm (de) synchronization and eeg single-trial classification of different motor imagery tasks. Neuroimage **31**(1), 153–159 (2006)
9. L.C. Cruikshank, A. Singhal, M. Hueppelsheuser, J.B. Caplan, Theta oscillations reflect a putative neural mechanism for human sensorimotor integration. J. Neurophysiol. **107**(1), 65–77 (2012). https://doi.org/10.1152/jn.00893.2010
10. S. Kurkin, S. Gordleeva, A. Savosenkov, N. Grigorev, N. Smirnov, V.V. Grubov, A. Udoratina, V. Maksimenko, V. Kazantsev, A.E. Hramov, Transcranial magnetic stimulation of the dorsolateral prefrontal cortex increases posterior theta rhythm and reduces latency of motor imagery. Sensors **23**(10), 4661 (2023)
11. M. Takemi, Y. Masakado, M. Liu, J. Ushiba, Event-related desynchronization reflects downregulation of intracortical inhibition in human primary motor cortex. J. Neurophysiol. **110**(5), 1158–1166 (2013)
12. S. Liburkina, A. Vasilyev, L. Yakovlev, S.Y. Gordleeva, A.Y. Kaplan, A motor imagery-based brain-computer interface with vibrotactile stimuli. Neurosci. Behav. Physiol. **48**, 1067–1077 (2018)
13. M. Wischnewski, Z.J. Haigh, S. Shirinpour, I. Alekseichuk, A. Opitz, The phase of sensorimotor mu and beta oscillations has the opposite effect on corticospinal excitability. Brain Stimul. **15**(5), 1093–1100 (2022)

14. C. Zrenner, P. Belardinelli, M. Ermolova, P.C. Gordon, M. Stenroos, B. Zrenner, U. Ziemann, μ-rhythm phase from somatosensory but not motor cortex correlates with corticospinal excitability in eeg-triggered tms. J. Neurosci. Methods **379**, 109662 (2022)

15. M. Lukoyanov, S.Y. Gordleeva, A. Pimashkin, N. Grigor'ev, A. Savosenkov, A. Motailo, V. Kazantsev, A.Y. Kaplan, The efficiency of the brain-computer interfaces based on motor imagery with tactile and visual feedback. Hum. Physiol. **44**, 280–288 (2018)

16. A.B. Remsik, L. Williams Jr., K. Gjini, K. Dodd, J. Thoma, T. Jacobson, M. Walczak, M. McMillan, S. Rajan, B.M. Young et al., Ipsilesional mu rhythm desynchronization and changes in motor behavior following post stroke bci intervention for motor rehabilitation. Front. Neurosci. **13**, 53 (2019)

17. L.M. Marques, A. Castellani, S.P. Barbosa, M. Imamura, L.R. Battistella, M. Simis, F. Fregni, Neuroplasticity changes in knee osteoarthritis (koa) indexed by event-related desynchronization/synchronization during a motor inhibition task. Somatosens. Mot. Res. (2023). https://doi.org/10.1080/08990220.2023.2188926

18. M. Lotze, K. Zentgraf, Contribution of the primary motor cortex to motor imagery. The neurophysiological foundations of mental and motor imagery **31**, 46 (2010)

19. B. Pelgrims, N. Michaux, E. Olivier, M. Andres, Contribution of the primary motor cortex to motor imagery: a sub-threshold tms study. Hum. Brain Mapp. **32**(9), 1471–1482 (2011)

20. K.R. Foysal, S.N. Baker, Induction of plasticity in the human motor system by motor imagery and transcranial magnetic stimulation. J. Physiol. **598**(12), 2385–2396 (2020)

21. E. Chew, W.-P. Teo, N. Tang, K.K. Ang, Y.S. Ng, J.H. Zhou, I. Teh, K.S. Phua, L. Zhao, C. Guan, Using transcranial direct current stimulation to augment the effect of motor imagery-assisted brain-computer interface training in chronic stroke patients-cortical reorganization considerations. Front. Neurol. **11**, 948 (2020)

22. K.J. Friston, Functional and effective connectivity: a review. Brain Connect. **1**(1), 13–36 (2011)

23. A.E. Hramov, N.S. Frolov, V.A. Maksimenko, S.A. Kurkin, V.B. Kazantsev, A.N. Pisarchik, Functional networks of the brain: from connectivity restoration to dynamic integration. Phys. Usp. **64**(6), 584 (2021)

24. S. Hétu, M. Grégoire, A. Saimpont, M.-P. Coll, F. Eugène, P.-E. Michon, P.L. Jackson, The neural network of motor imagery: an ale meta-analysis. Neurosci. Biobehav. Rev. **37**(5), 930–949 (2013)

25. A. Guillot, C. Collet, V.A. Nguyen, F. Malouin, C. Richards, J. Doyon, Functional neuroanatomical networks associated with expertise in motor imagery. Neuroimage **41**(4), 1471–1483 (2008)

26. H. Yu, S. Ba, Y. Guo, L. Guo, G. Xu, Effects of motor imagery tasks on brain functional networks based on eeg mu/beta rhythm. Brain Sci. **12**(2), 194 (2022)

27. A. Solodkin, P. Hlustik, E.E. Chen, S.L. Small, Fine modulation in network activation during motor execution and motor imagery. Cereb. Cortex **14**(11), 1246–1255 (2004)

28. H. Chen, Q. Yang, W. Liao, Q. Gong, S. Shen, Evaluation of the effective connectivity of supplementary motor areas during motor imagery using granger causality mapping. Neuroimage **47**(4), 1844–1853 (2009)

29. S. Kurkin, A. Badarin, V. Grubov, V. Maksimenko, A. Hramov, The oxygen saturation in the primary motor cortex during a single hand movement: functional near-infrared spectroscopy (fnirs) study. Eur. Phys. J. Plus **136**(5), 548 (2021)

30. A. Hyvärinen, E. Oja, Independent component analysis: algorithms and applications. Neural Netw. **13**(4–5), 411–430 (2000). https://doi.org/10.1016/S0893-6080(00)00026-5

31. E. Maris, R. Oostenveld, Nonparametric statistical testing of eeg-and meg-data. J. Neurosci. Methods **164**(1), 177–190 (2007). https://doi.org/10.1016/j.jneumeth.2007.03.024

32. J.-M. Schoffelen, J. Gross, Source connectivity analysis with meg and eeg. Hum. Brain Mapp. **30**(6), 1857–1865 (2009)

33. R. Grech, T. Cassar, J. Muscat, K.P. Camilleri, S.G. Fabri, M. Zervakis, P. Xanthopoulos, V. Sakkalis, B. Vanrumste, Review on solving the inverse problem in eeg source analysis. J. Neuroeng. Rehabil. **5**(1), 1–33 (2008)

34. C.J. Holmes, R. Hoge, L. Collins, R. Woods, A.W. Toga, A.C. Evans, Enhancement of mr images using registration for signal averaging. J. Comput. Assist. Tomogr. **22**(2), 324–333 (1998)

35. M. Fuchs, J. Kastner, M. Wagner, S. Hawes, J.S. Ebersole, A standardized boundary element method volume conductor model. Clin. Neurophysiol. **113**(5), 702–712 (2002)

36. N. Tzourio-Mazoyer, B. Landeau, D. Papathanassiou, F. Crivello, O. Etard, N. Delcroix, B. Mazoyer, M. Joliot, Automated anatomical labeling of activations in spm using a macroscopic anatomical parcellation of the mni mri single-subject brain. Neuroimage **15**(1), 273–289 (2002)

37. A.M. Bastos, J.-M. Schoffelen, A tutorial review of functional connectivity analysis methods and their interpretational pitfalls. Front. Syst. Neurosci. **9**, 175 (2016)

38. A. Zalesky, A. Fornito, E.T. Bullmore, Network-based statistic: identifying differences in brain networks. Neuroimage **53**(4), 1197–1207 (2010)

39. C.R. Genovese, N.A. Lazar, T. Nichols, Thresholding of statistical maps in functional neuroimaging using the false discovery rate. Neuroimage **15**(4), 870–878 (2002)

40. D.S. Bassett, O. Sporns, Network neuroscience. Nat. Neurosci. **20**(3), 353–364 (2017)

41. R. Oostenveld, P. Fries, E. Maris, J.-M. Schoffelen, Fieldtrip: open source software for advanced analysis of meg, eeg, and invasive electrophysiological data. Comput. Intell. Neurosci. **2011**, 1–9 (2011)

42. N. Sharma, J.-C. Baron, Does motor imagery share neural networks with executed movement: a multivariate fmri analysis. Front. Hum. Neurosci. **7**, 564 (2013)

43. F. Li, C. Yi, L. Song, Y. Jiang, W. Peng, Y. Si, T. Zhang, R. Zhang, D. Yao, Y. Zhang et al., Brain network reconfiguration during motor imagery revealed by a large-scale network analysis of scalp eeg. Brain Topogr. **32**, 304–314 (2019)
44. G. Pfurtscheller, C. Neuper, Motor imagery activates primary sensorimotor area in humans. Neurosci. Lett. **239**(2–3), 65–68 (1997)
45. A.C. Chen, W. Feng, H. Zhao, Y. Yin, P. Wang, Eeg default mode network in the human brain: spectral regional field powers. Neuroimage **41**(2), 561–574 (2008)
46. K.J. Miller, G. Schalk, E.E. Fetz, M. Den Nijs, J.G. Ojemann, R.P. Rao, Cortical activity during motor execution, motor imagery, and imagery-based online feedback. Proc. Natl. Acad. Sci. **107**(9), 4430–4435 (2010)
47. J. Xie, M. Peng, J. Lu, C. Xiao, X. Zong, M. Wang, D. Gao, Y. Qin, T. Liu, Enhancement of event-related desynchronization in motor imagery based on transcranial electrical stimulation. Front. Hum. Neurosci. **15**, 635351 (2021)
48. S. Asuga, Y. Matsushika, Y. Kasashima-Shindo, D. Kamatani, T. Fujiwara, M. Liu, J. Ushiba, Transcranial direct current stimulation enhances mu rhythm desynchronization during motor imagery that depends on handedness. Laterality **20**(4), 453–468 (2015)
49. Y.Y. Chen, K.J. Lambert, C.R. Madan, A. Singhal, Mu oscillations and motor imagery performance: a reflection of intra-individual success, not inter-individual ability. Hum. Mov. Sci. **78**, 102819 (2021)
50. T. Gao, Y. Hu, J. Zhuang, Y. Bai, R. Lu, Repetitive transcranial magnetic stimulation of the brain region activated by motor imagery involving a paretic wrist and hand for upper-extremity motor improvement in severe stroke: A preliminary study. Brain Sci. **13**(1), 69 (2022)
51. F. Grami, G. De Marco, F. Bodranghien, M. Manto, C. Habas, Cerebellar transcranial direct current stimulation reconfigurates static and dynamic functional connectivity of the resting-state networks. Cerebellum ataxias **8**(1), 1–12 (2021)
52. S. Sawai, S. Murata, S. Fujikawa, R. Yamamoto, K. Shima, H. Nakano, Effects of neurofeedback training combined with transcranial direct current stimulation on motor imagery: a randomized controlled trial. Front. Neurosci. **17**, 299 (2023)
53. E. Saruco, F. Di Rienzo, S. Nunez-Nagy, M.A. Rubio-Gonzalez, P.L. Jackson, C. Collet, A. Saimpont, A. Guillot, Anodal tdcs over the primary motor cortex improves motor imagery benefits on postural control: a pilot study. Sci. Rep. **7**(1), 480 (2017)
54. R.M. Hardwick, S. Caspers, S.B. Eickhoff, S.P. Swinnen, Neural correlates of action: comparing meta-analyses of imagery, observation, and execution. Neurosci. Biobehav. Rev. **94**, 31–44 (2018). https://doi.org/10.1016/j.neubiorev.2018.08.003
55. N. Mizuguchi, H. Nakata, T. Hayashi, M. Sakamoto, T. Muraoka, Y. Uchida, K. Kanosue, Brain activity during motor imagery of an action with an object: a functional magnetic resonance imaging study. Neurosci. Res. **76**(3), 150–155 (2013)
56. S.A. Huettel, J. Misiurek, Modulation of prefrontal cortex activity by information toward a decision rule. NeuroReport **15**(12), 1883–1886 (2004)
57. A. Genovesio, P.J. Brasted, A.R. Mitz, S.P. Wise, Prefrontal cortex activity related to abstract response strategies. Neuron **47**(2), 307–320 (2005)
58. G. Rainer, W.F. Asaad, E.K. Miller, Selective representation of relevant information by neurons in the primate prefrontal cortex. Nature **393**(6685), 577–579 (1998)